Electronic Supplementary Material (ESI) for Inorganic Chemistry Frontiers.

Supplementary data

Mixed anion/cation redox in $K_{0.78}Fe_{1.60}S_2$ for a high-performance cathode in potassium ion batteries

Su Cheol Han,‡[a] Woon Bae Park,‡[a] Kee-Sun Sohn*[b] and Myoungho Pyo*[a]

[a] *Department of Printed Electronics Engineering, Sunchon National University, Sunchon, Chonnam 57922,*

Republic of Korea. E-mail: mho@sunchon.ac.kr

[b] *Faculty of Nanotechnology and Advanced Materials Engineering, Sejong University, Seoul 05006,*

Republic of Korea. E-mail: kssohn@sejong.ac.kr

‡ These authors contributed equally to this work.

List of contents

Fig. S1 EDX maps and spectra of (A) charged and (B) discharged $K_{0.78}Fe_{1.60}S_2$

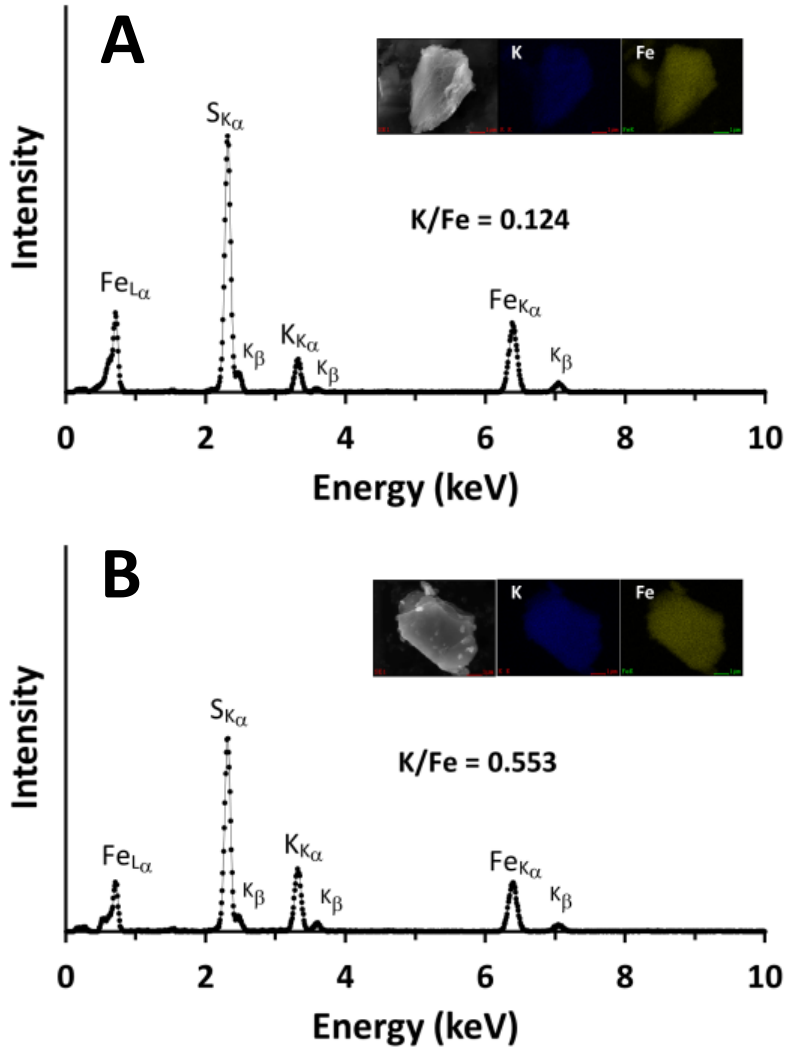

Fig. S2 XPS spectra of half-charged $K_{0.78}Fe_{1.60}S_2$. The spectra reveals that the charge accompanies simultaneous oxidation of Fe(II) and S^{2-}.

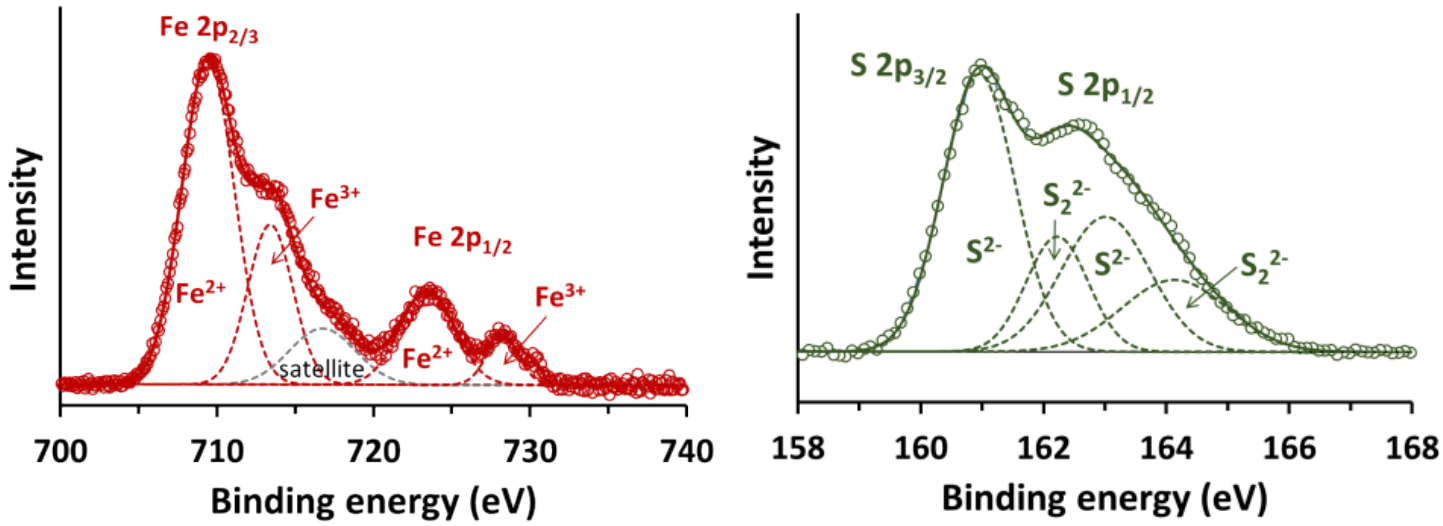

Fig. S3 Full in-situ XRD patterns during the 1st C/D of $K_{0.78}Fe_{1.60}S_2$.

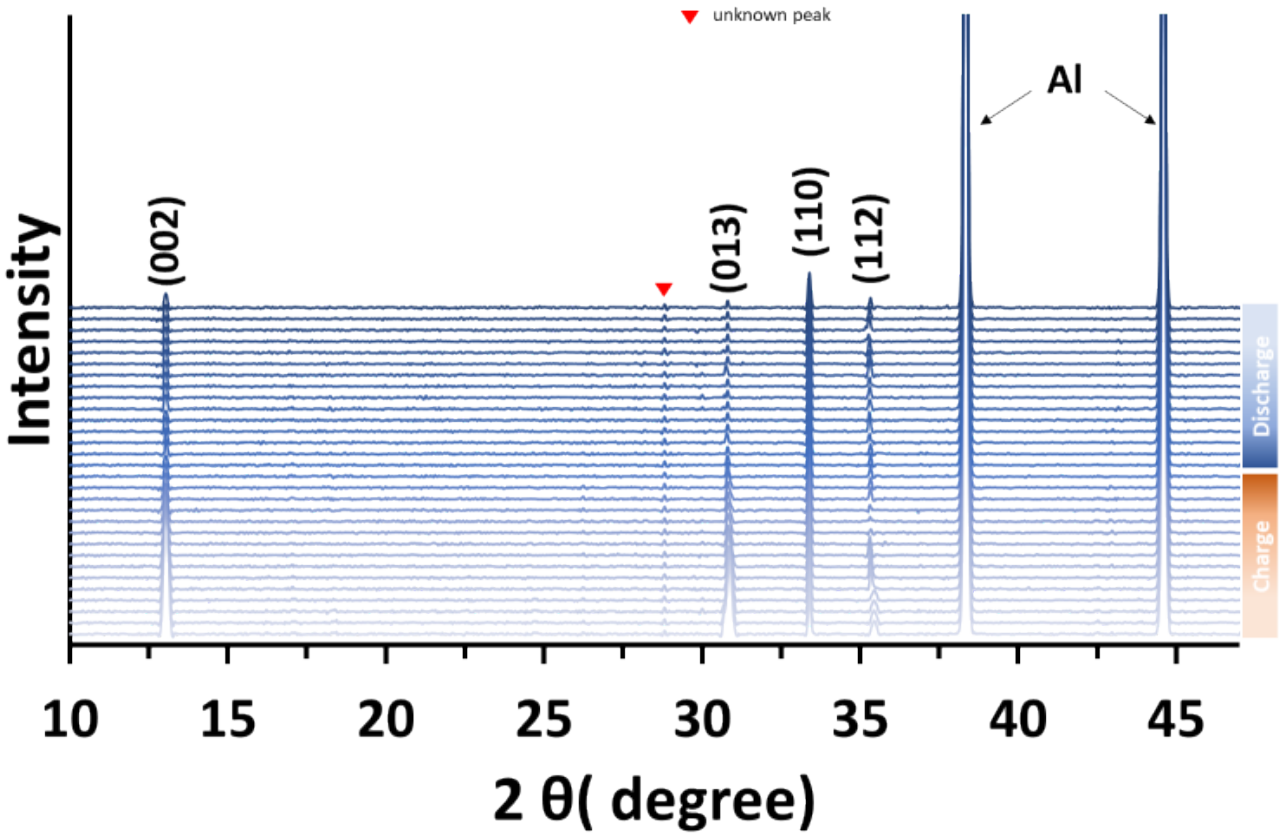

Table S1 Summary of DFT calculation results for 161 configurations.

Supercell No.	VASP energy(eV)	*Bandgap type	Total Bandgap(eV)
1	-172.794469	I	0.316
2	-172.563275	D	0.280
3	-172.757400	I	0.301
4	-172.517168	I	0.337
5	-172.732480	I	0.354
6	-172.690145	I	0.282
7	-172.800289	I	0.279
8	-173.304633	I	0.511
9	-172.845096	D	0.293
10	-173.319979	D	0.782
11	-172.586786	I	0.364
12	-173.213713	D	0.617
13	-172.781588	I	0.353
14	-173.241291	I	0.680
15	-172.742485	D	0.358
16	-173.248933	D	0.448
17	-172.513452	D	0.374
18	-173.355325	I	0.758
19	-173.238444	I	0.664
20	-172.702348	I	0.390
21	-172.657223	I	0.282
22	-172.471387	I	0.358
23	-172.833554	I	0.303
24	-172.688943	D	0.366
25	-173.372098	D	0.813
26	-172.791298	I	0.268
27	-172.570008	D	0.416
28	-172.827593	I	0.283
29	-172.786428	I	0.311
30	-172.517227	I	0.369
31	-172.707901	I	0.357
32	-172.537918	I	0.390
33	-173.217347	I	0.689
34	-172.673665	I	0.274
35	-173.093225	D	0.375
36	-173.370872	I	0.808
37	-172.450951	D	0.397
38	-172.794141	D	0.366
39	-172.738561	D	0.359
40	-172.742345	D	0.366
41	-172.760442	I	0.267
42	-173.272883	D	0.862
43	-172.473482	I	0.283
44	-173.263523	I	0.500
45	-170.638650	I	0.000
46	-170.946143	I	0.000
47	-170.476569	I	0.874
48	-171.122553	I	0.626
49	-170.484864	I	0.000
50	-171.335331	I	0.784
51	-170.578460	MM	
52	-170.047491	I	0.000
53	-171.289918	I	0.751
54	-170.326907	MM	
55	-170.563609	I	0.000
56	-170.727715	I	0.597
57	-170.362493	I	0.000
58	-170.288951	MM	
59	-170.624089	I	0.548
60	-170.820380	MM	
61	-170.710600	MM	
62	-170.278581	MM	
63	-172.795480	I	0.384
64	-172.708923	I	0.324
65	-173.151347	D	0.609
66	-172.570623	D	0.388
67	-173.270650	I	0.603
68	-172.688134	I	0.414
69	-173.263816	D	0.600
70	-173.273131	I	0.450
71	-172.866800	D	0.310
72	-173.332993	D	0.666
73	-173.253054	D	0.771
74	-172.781227	D	0.361
75	-172.755962	D	0.321
76	-173.136924	D	0.748
77	-172.483943	I	0.338
78	-173.470288	D	0.895
79	-171.020328	MM	
80	-170.521185	MM	
81	-170.898735	MM	
82	-170.576882	I	0.000
83	-171.237315	D	0.528
84	-171.099646	I	0.672
85	-171.142724	I	0.668
86	-170.940539	MM	
87	-170.987733	I	0.527
88	-170.689063	I	0.332
89	-173.149569	I	0.211
90	-172.679988	MM	
91	-172.248640	MM	
92	-173.195711	D	0.172
93	-172.791984	MM	
94	-173.226819	I	0.324
95	-172.491530	I	0.154
96	-172.989819	I	0.369
97	-173.080514	I	0.227
98	-173.320510	D	0.593
99	-172.424863	MM	
100	-172.710805	I	0.126
101	-173.119070	I	0.071
102	-172.952172	I	0.319
103	-172.482275	I	0.165
104	-173.154162	D	0.171
105	-172.876819	I	0.075
106	-173.142482	I	0.188
107	-172.212731	I	0.000
108	-172.779149	I	0.071
109	-172.819793	MM	
110	-173.173959	I	0.201
111	-172.636334	I	0.132
112	-172.394311	MM	
113	-173.061556	I	0.346
114	-172.782305	I	0.308
115	-172.541374	I	0.159
116	-173.416481	D	0.743
117	-173.049302	D	0.301
118	-173.387047	D	0.783
119	-172.538186	I	0.063
120	-173.144586	I	0.297
121	-172.430092	MM	
122	-173.118980	I	0.166
123	-172.708731	MM	
124	-173.142973	I	0.086
125	-172.837015	MM	
126	-173.170710	D	0.190
127	-172.794169	I	0.287
128	-173.246998	I	0.513
129	-172.705268	I	0.136
130	-172.934492	I	0.186
131	-173.174377	I	0.181
132	-172.946475	I	0.198
133	-172.745582	I	0.277
134	-173.173524	D	0.160
135	-172.497043	MM	
136	-173.188443	D	0.207
137	-172.724896	I	0.049
138	-172.920596	I	0.292
139	-172.671997	D	0.277
140	-173.013008	D	0.414
141	-172.983175	I	0.539
142	-173.040030	I	0.345
143	-172.910824	I	0.397
144	-173.282818	D	0.449
145	-173.245419	D	0.458
146	-173.268728	D	0.417
147	-172.725880	D	0.297
148	-171.007850	I	0.273
149	-170.759859	I	0.000
150	-170.974174	I	0.277
151	-171.306659	I	0.347
152	-170.762469	I	0.131
153	-170.894067	MM	
154	-170.197650	MM	
155	-173.046075	I	0.316
156	-173.106126	D	0.650
157	-172.633507	D	0.208
158	-173.359521	I	0.717
159	-173.042660	D	0.289
160	-173.468995	I	0.806
161	-172.541248	I	0.024

* D = direct; I = indirect; MM = magnetic metal.

Fig. S4 DFT-calculated band structures and the orbital-projected PDOS.

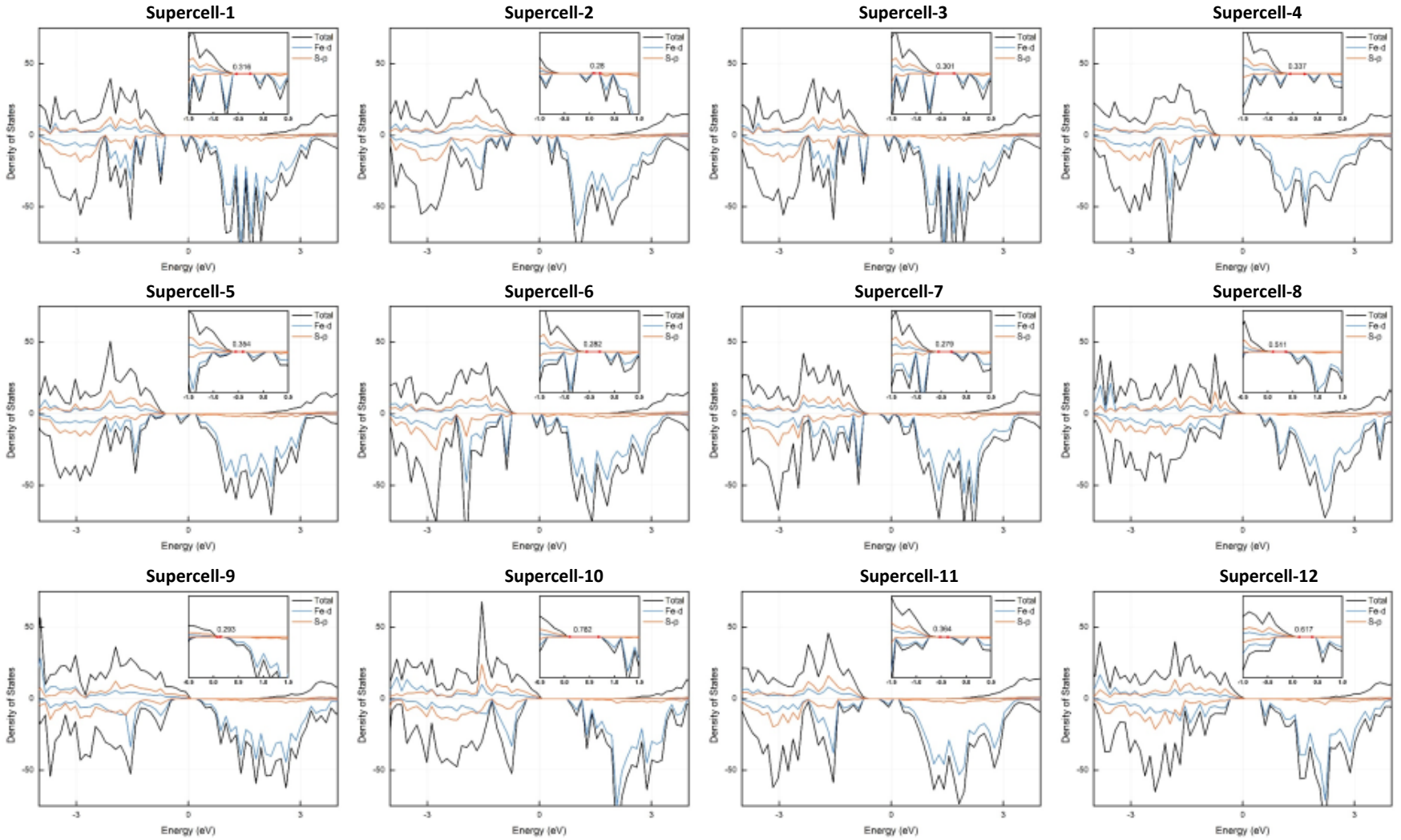

Fig. S4 (continued) DFT-calculated band structures and the orbital-projected PDOS.

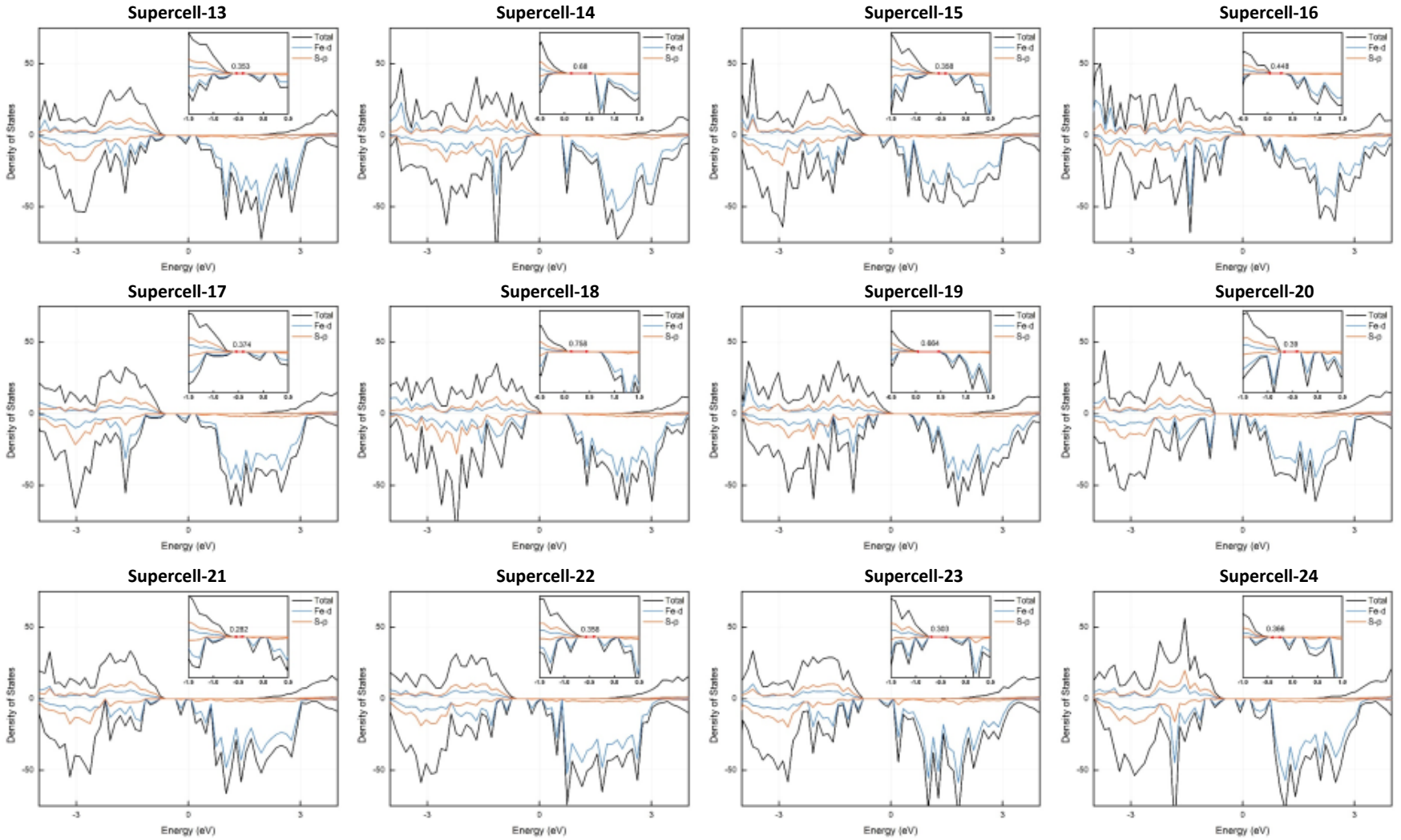

Fig. S4 (continued) DFT-calculated band structures and the orbital-projected PDOS.

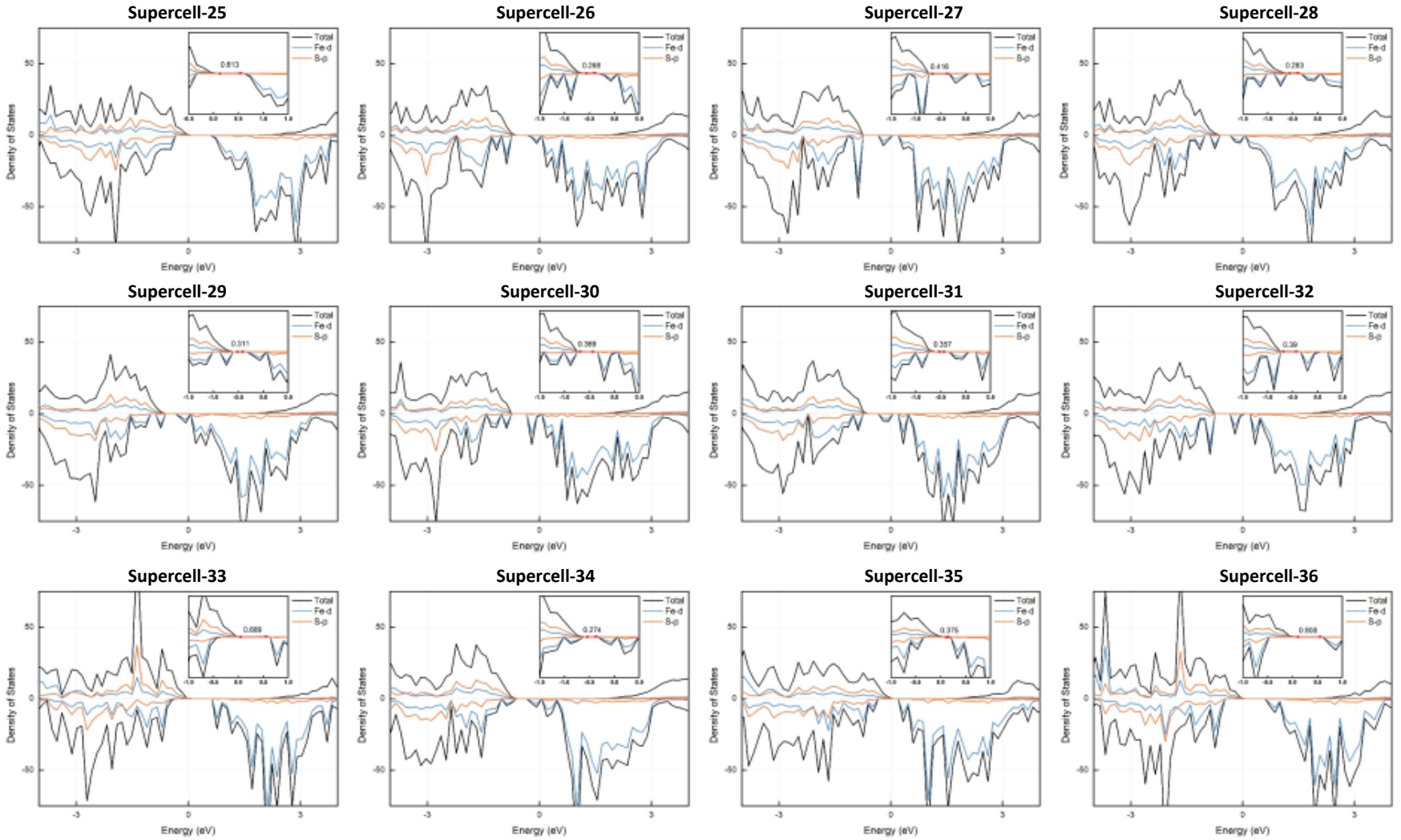

Fig. S4 (continued) DFT-calculated band structures and the orbital-projected PDOS.

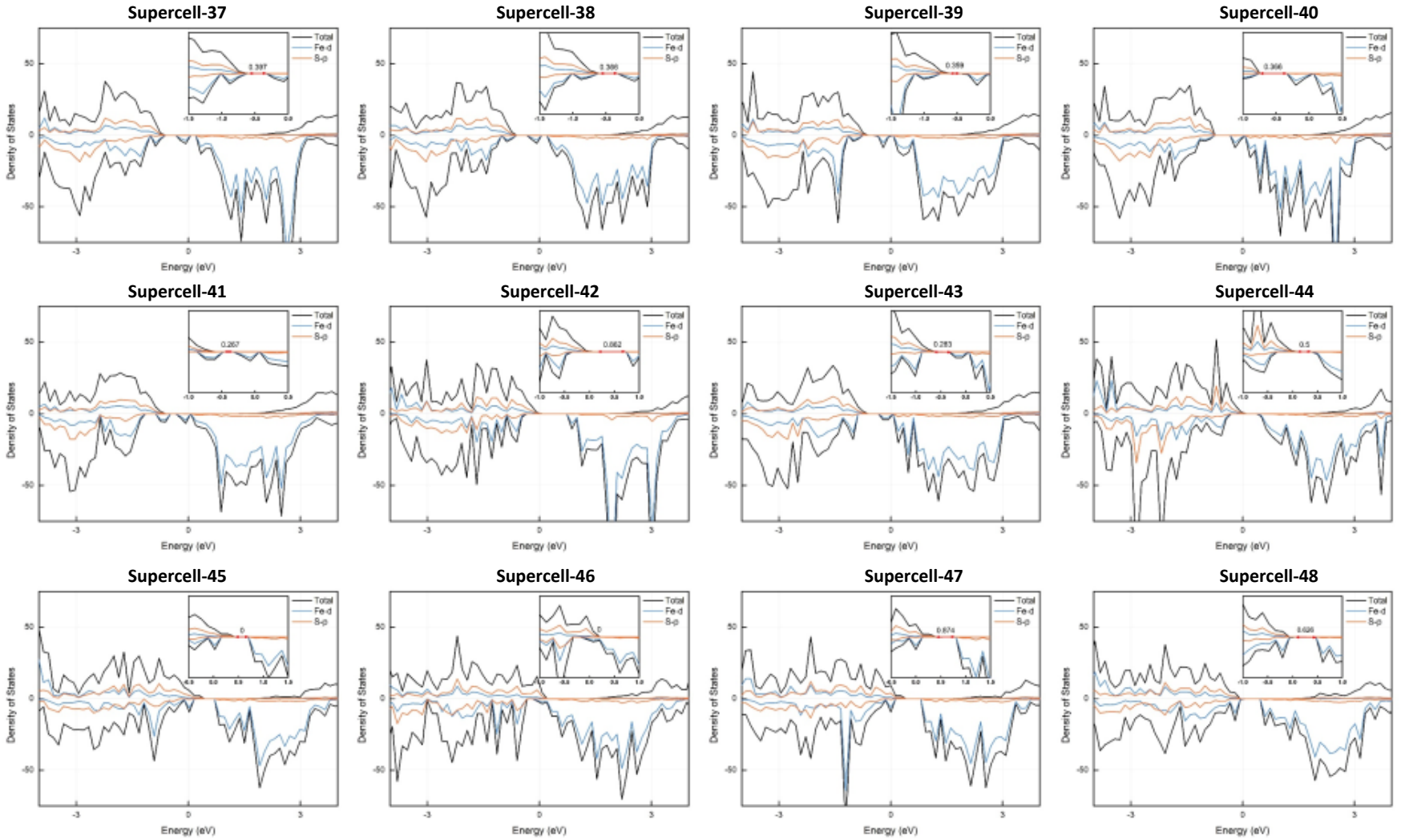

Fig. S4 (continued) DFT-calculated band structures and the orbital-projected PDOS.

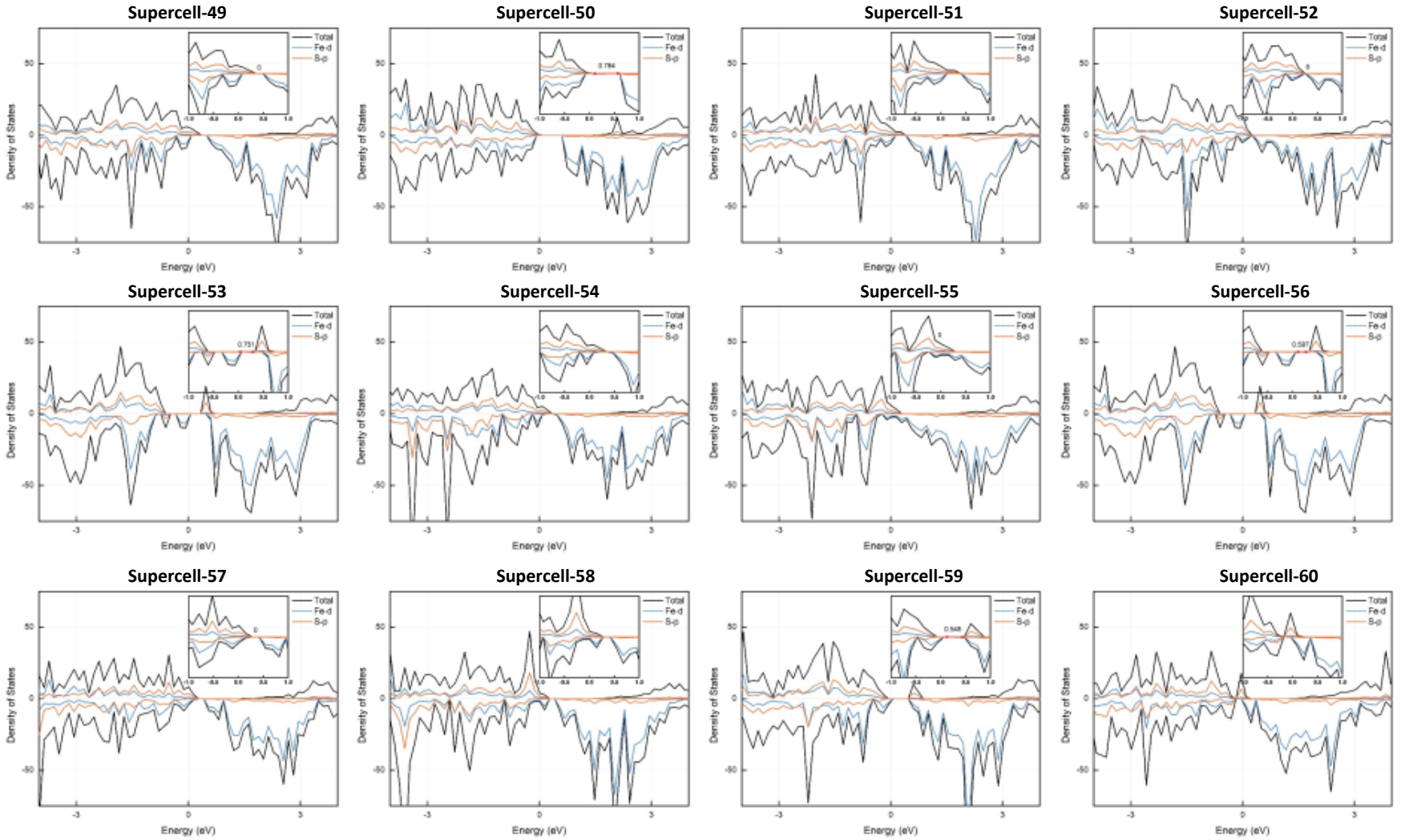

Fig. S4 (continued) DFT-calculated band structures and the orbital-projected PDOS.

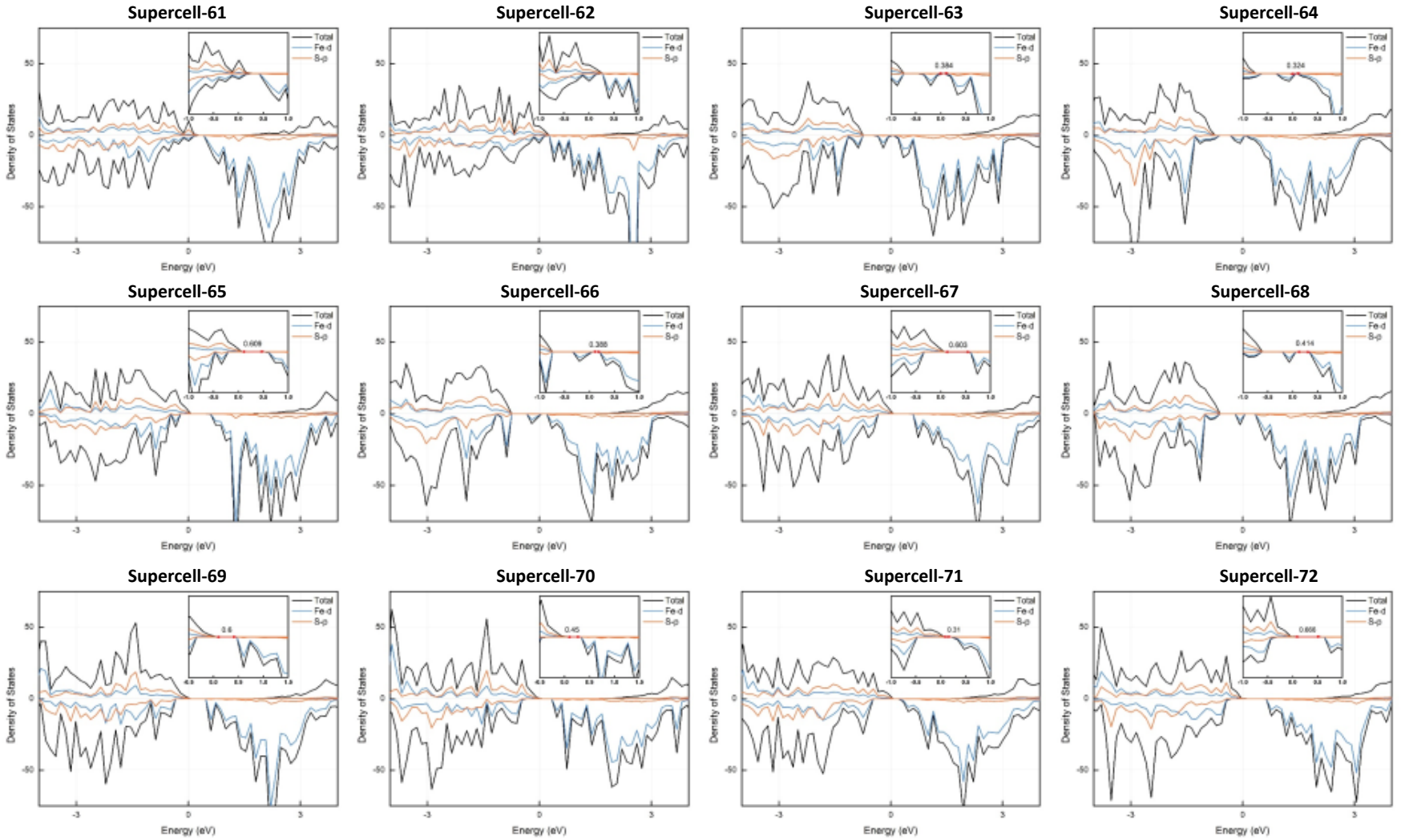

Fig. S4 (continued) DFT-calculated band structures and the orbital-projected PDOS.

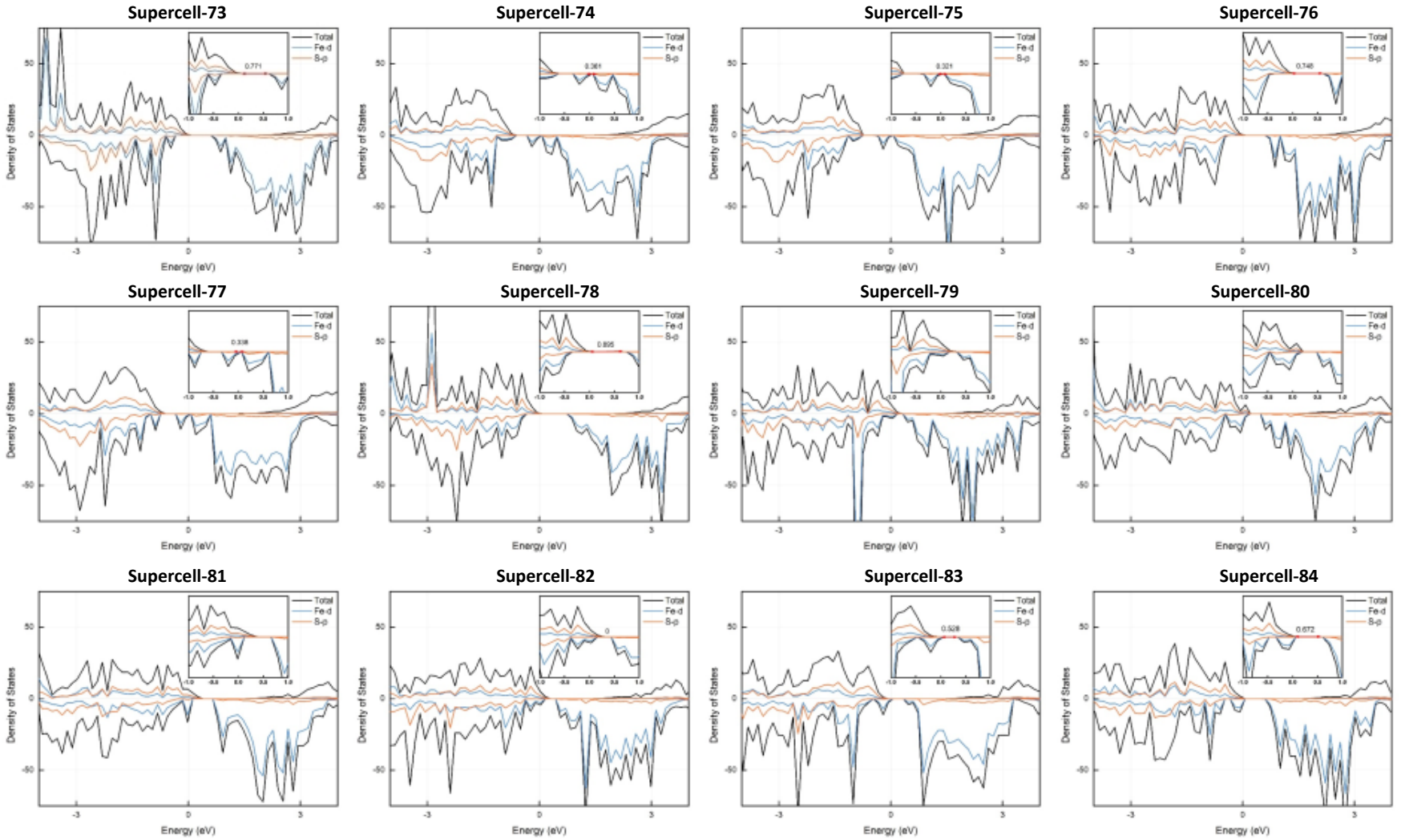

Fig. S4 (continued) DFT-calculated band structures and the orbital-projected PDOS.

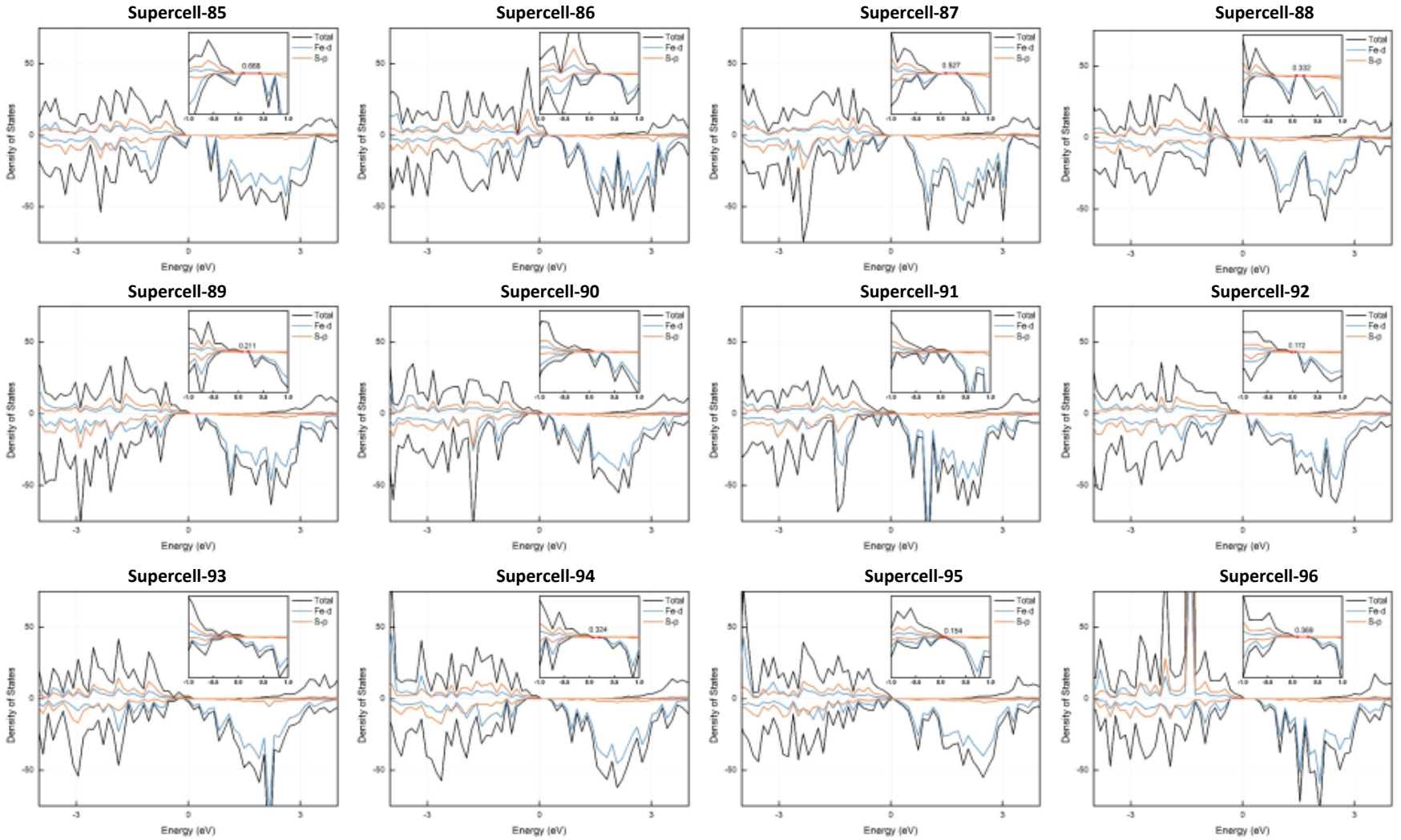

Fig. S4 (continued) DFT-calculated band structures and the orbital-projected PDOS.

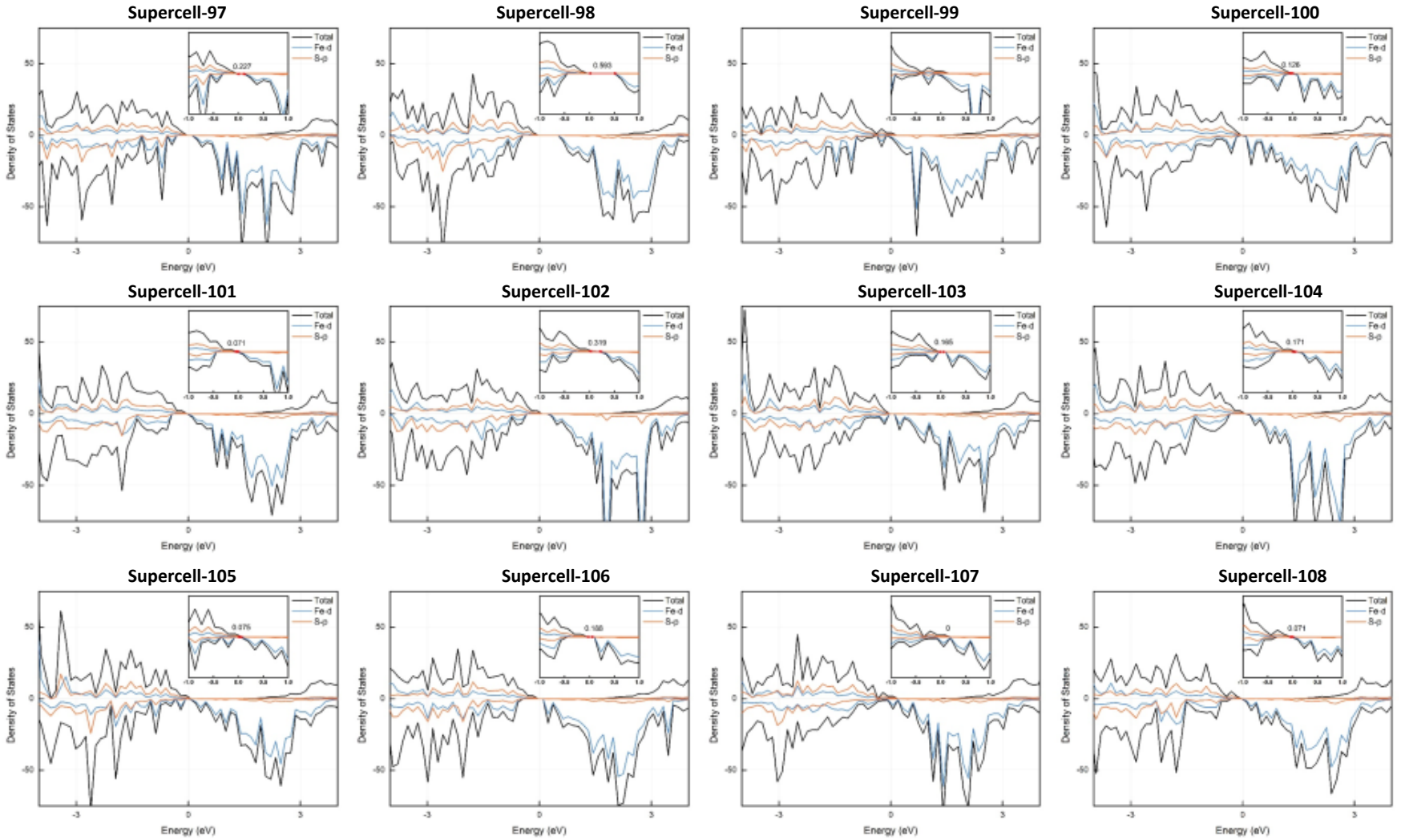

Fig. S4 (continued) DFT-calculated band structures and the orbital-projected PDOS.

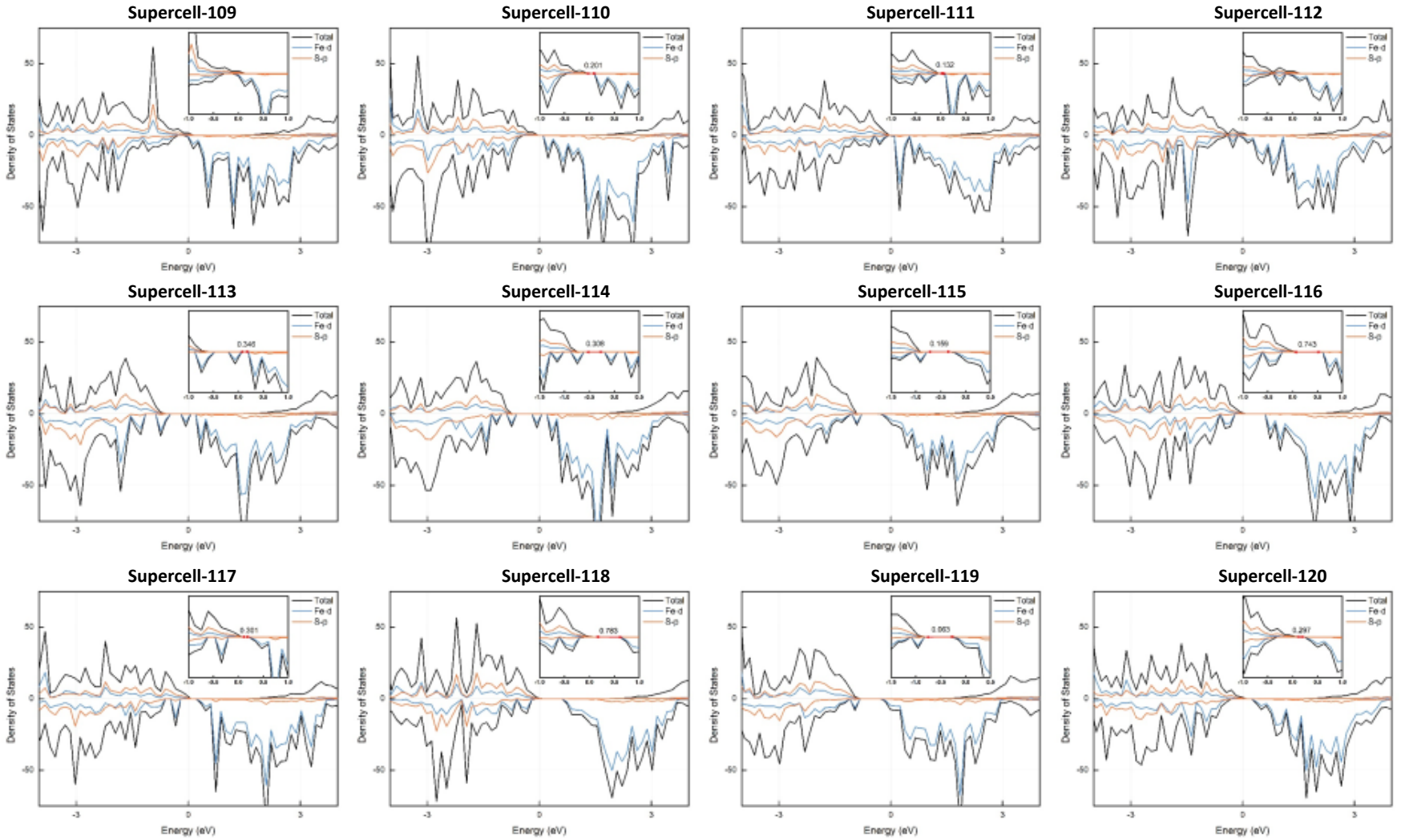

Fig. S4 (continued) DFT-calculated band structures and the orbital-projected PDOS.

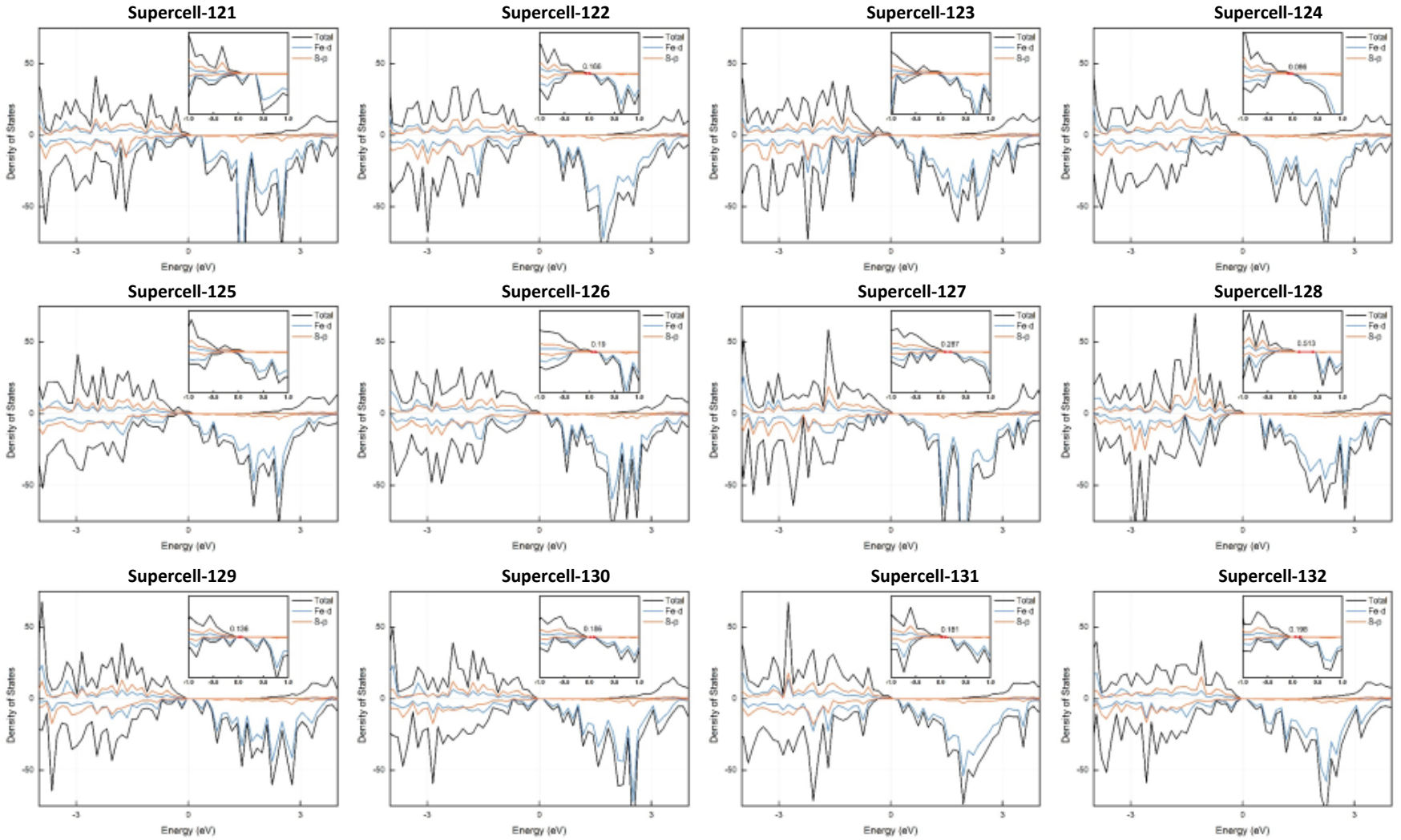

Fig. S4 (continued) DFT-calculated band structures and the orbital-projected PDOS.

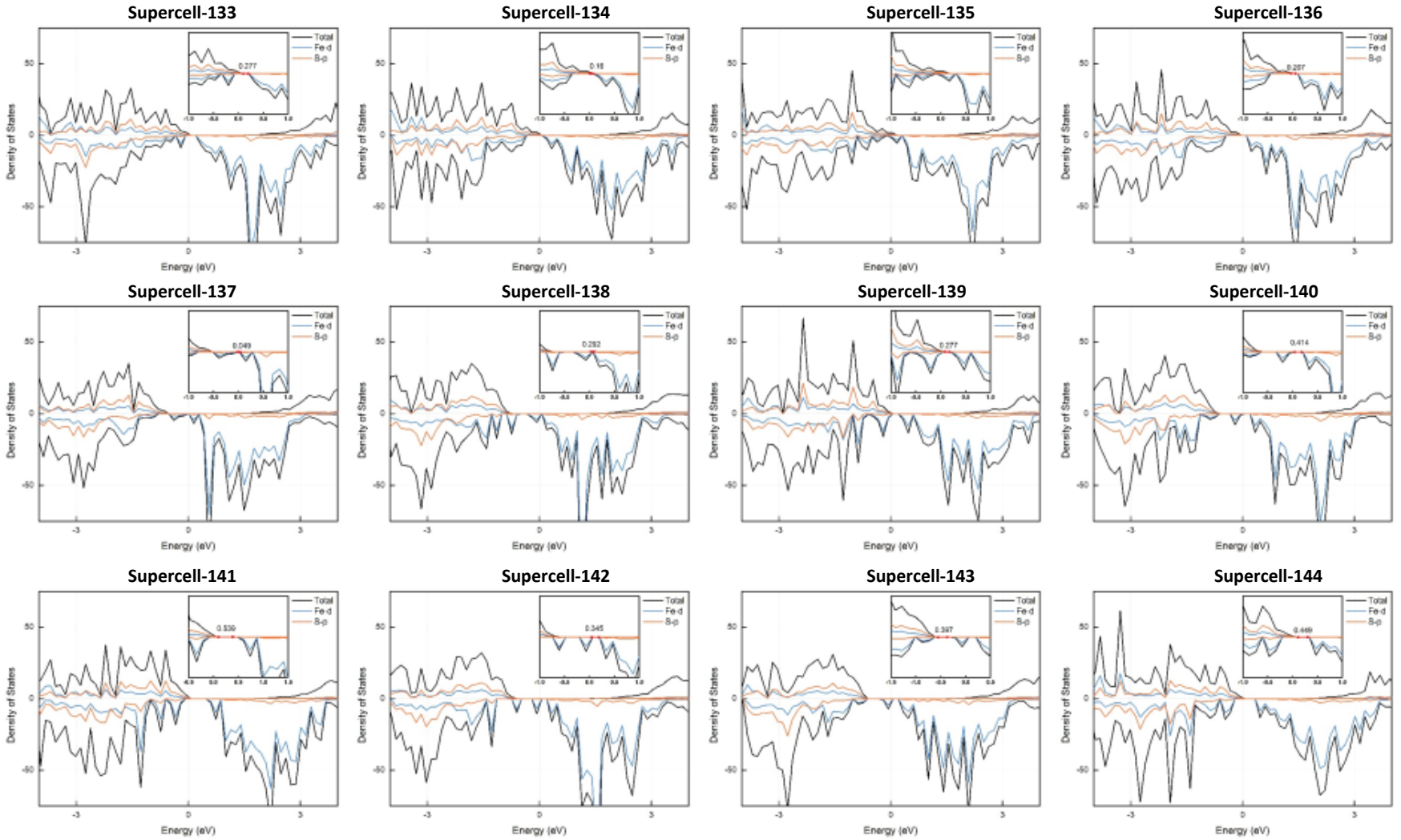

Fig. S4 (continued) DFT-calculated band structures and the orbital-projected PDOS.

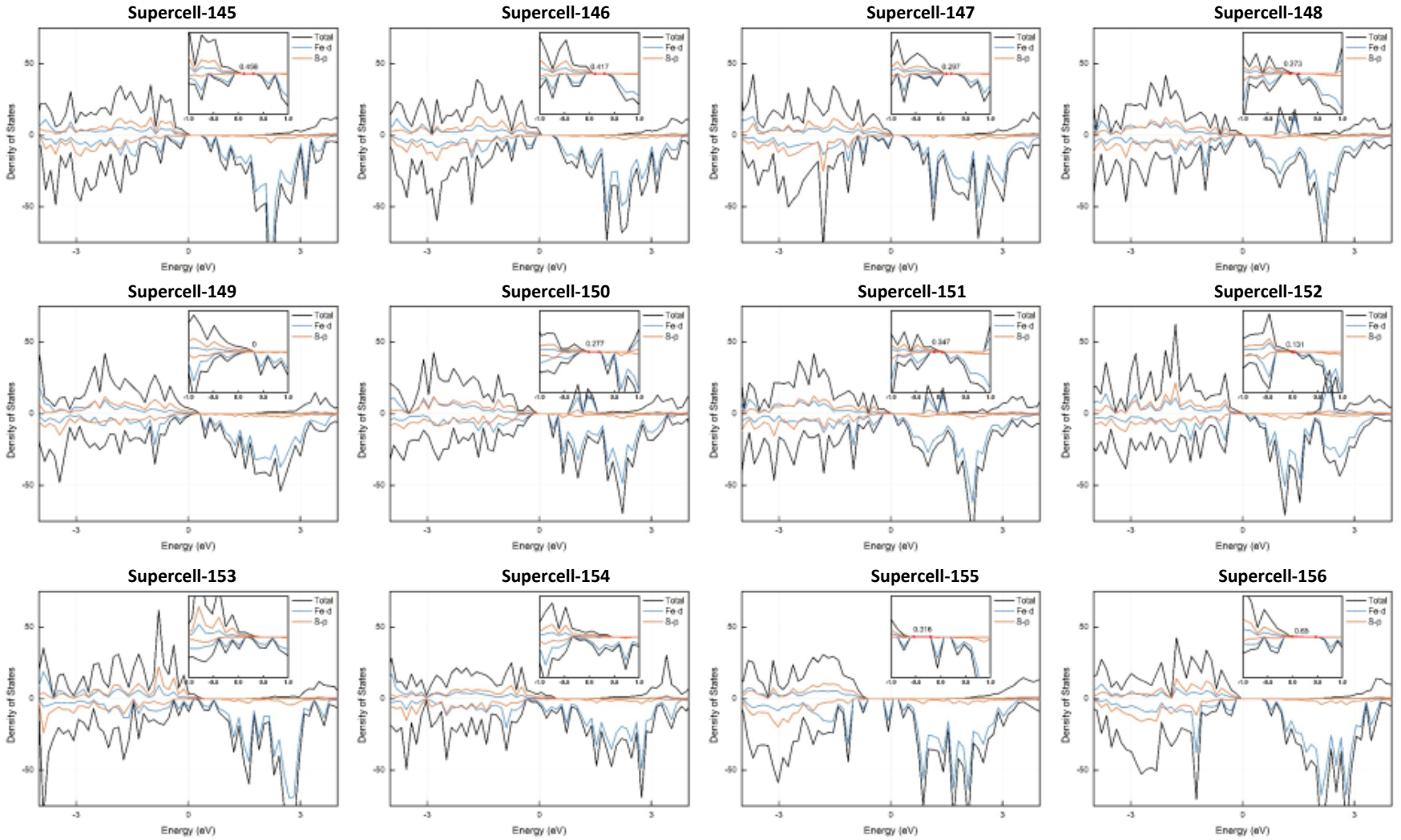

Fig. S4 (continued) DFT-calculated band structures and the orbital-projected PDOS.

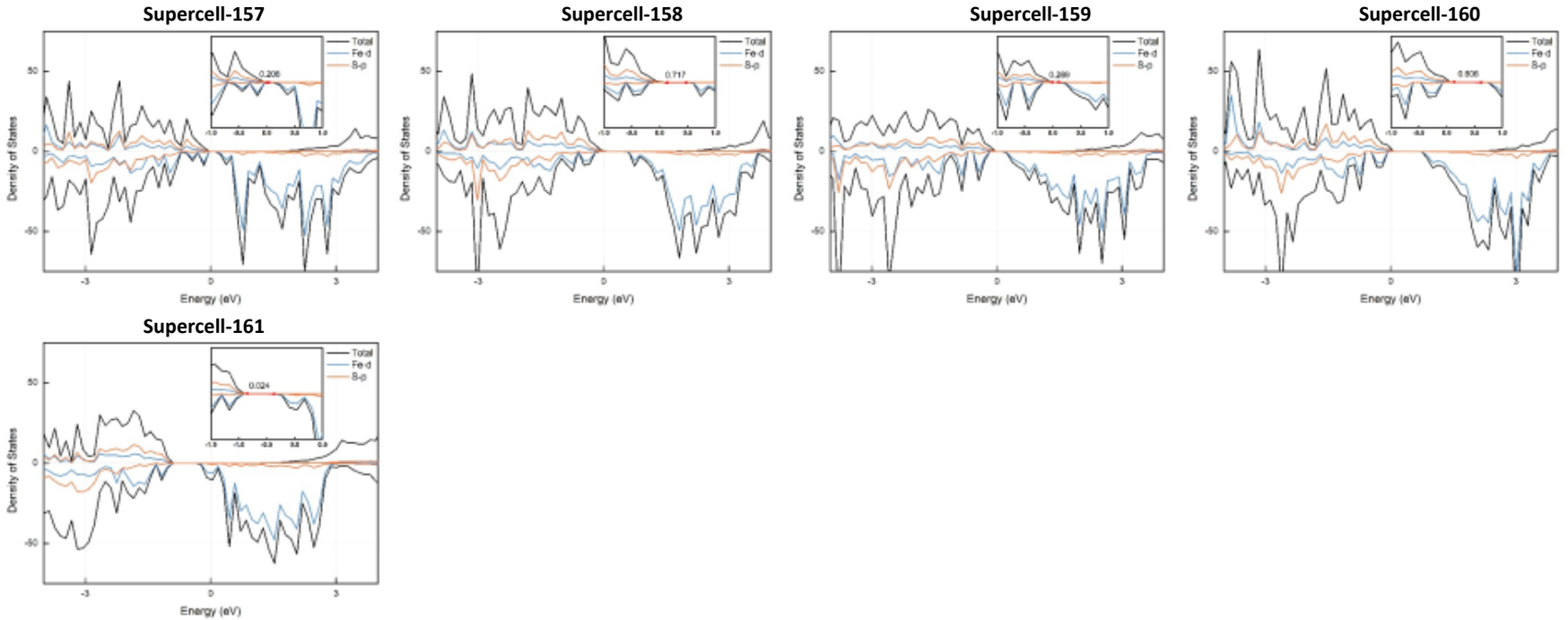

Fig. S5 Cycle stability and Coulombic efficiency during 100 C/D cycles at 20mAg^{-1}